Journal of Medicinal Chemistry

ARTICLE

pubs.acs.org/jmc

Novel Nitric Oxide-Releasing Derivatives of Farnesylthiosalicylic Acid: Synthesis and Evaluation of Antihepatocellular Carcinoma Activity

Yong Ling,[†,‡,⊥] Xiaolei Ye,[§,⊥] Zhenzhen Zhang,[†] Yihua Zhang,[*,†] Yisheng Lai,[†] Hui Ji,[*,†] Sixun Peng,[†] and Jide Tian[∥]

[†]Center of Drug Discovery, China Pharmaceutical University, Nanjing 210009, People's Republic of China

[‡]Medical College, Nantong University, Nantong 226001, People's Republic of China

[§]Ningbo Institute of Medical Sciences, Ningbo University, Ningbo 315000, People's Republic of China

[∥]Department of Molecular and Medical Pharmacology, University of California—Los Angeles, Los Angeles, California 90095, United States

Supporting Information

ABSTRACT: Novel furoxan-based nitric oxide (NO) releasing derivatives (**8a**−**p**) of farnesylthiosalicylic acid (FTS) were synthesized. Compound **8l** displayed the strongest inhibition on the proliferation of human hepatocellular carcinoma (HCC) cells in vitro, superior to FTS, sorafenib, and furoxan moiety, selectively induced high frequency of HCC cell apoptosis, and produced high levels of NO in HCC cells but not in nontumor liver cells. Furthermore, **8l** exhibited low acute toxicity to mice and significantly inhibited the growth of HCC tumors in vivo and the Ras-related signaling in the tumors. Therefore, our novel findings may provide a new framework for the design of new NO-releasing furoxan/FTS hybrids for the intervention of human HCC.

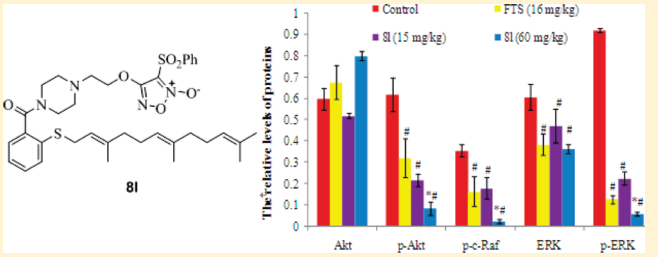

INTRODUCTION

Human hepatocellular carcinoma (HCC) is the sixth most frequent cancer worldwide.[1] The aberrant activation of oncogenes, such as the Ras, likely contributes to the development of HCC.[2] The Ras proteins are membrane-anchored guanine-nucleotide binding proteins and function as biological switches that can mediate signal transduction between G-protein-coupled receptors and downstream events, such as mitogen-activated protein kinase (MAPK) and Akt.[3,4] The activation of MAPK and Akt signaling regulates cell proliferation, migration, differentiation, and apoptosis.[5−9] Notably, the mutations of the Ras genes usually result in the constitutive activation of Ras-GTP (guanosine triphosphate) proteins and overstimulation of downstream signaling, promoting the development and progression of tumors in human.[10] Previous studies have shown that Ras mutations occur in human HCC and human hepatoma cell lines,[11,12] and Ras and related signaling regulate the development and progression of HCC.[13,14] Given that there is no effective chemotherapy for HCC, the development of new therapeutic agents that inhibit the Ras-related signaling pathway will be of great significance.

Farnesylthiosalicylic acid (FTS), a novel Ras inhibitor, structurally resembles the carboxyl-terminal farnesylcysteine group, similar to all Ras proteins. FTS can dislodge the Ras protein from its anchorage domains and facilitate its degradation, thus reducing cellular Ras content, and functions as a Ras antagonist in cells, inhibiting tumor cell proliferation.[15−18] The potential of FTS for the treatment of human HCC has been tested; however, its therapeutic efficacy is limited.[19] Therefore, development of novel Ras inhibitors with potent anti-HCC activity is of pharmaceutical importance.

High levels of nitric oxide (NO) and its metabolic derivatives, the reactive nitrogen species (RNS) and reactive oxygen species (ROS), can modify functional proteins by S-nitrosylation, nitration, and disulfide formation, leading to bioregulation, inactivation and cytotoxicity, particularly in tumor cells.[20] Indeed, previous studies have shown that the synthesized NO-releasing compounds have strong cytotoxicity against human carcinoma cells in vitro and inhibit cancer growth and metastasis in vivo.[21−23] Furoxans are thermally stable compounds and represent an important class of NO donors, which can produce high levels of NO in vitro and inhibit the growth of tumors in vivo.[24−26] Our previous studies have developed a number of promising furoxan-based NO releasing anticancer drug candidates that have selective cytotoxicity against HCC cells.[24,27,28] Given that FTS can inhibit the Ras-related signaling and sensitize tumor cells to apoptotic inducers, we hypothesized that novel types of furoxan/FTS hybrids could inhibit the Ras-related signaling and tumor cell proliferation and produce high levels of NO, leading to

Received: December 4, 2010
Published: April 19, 2011

Scheme 1. Synthesis of Compounds 8a−p[a]

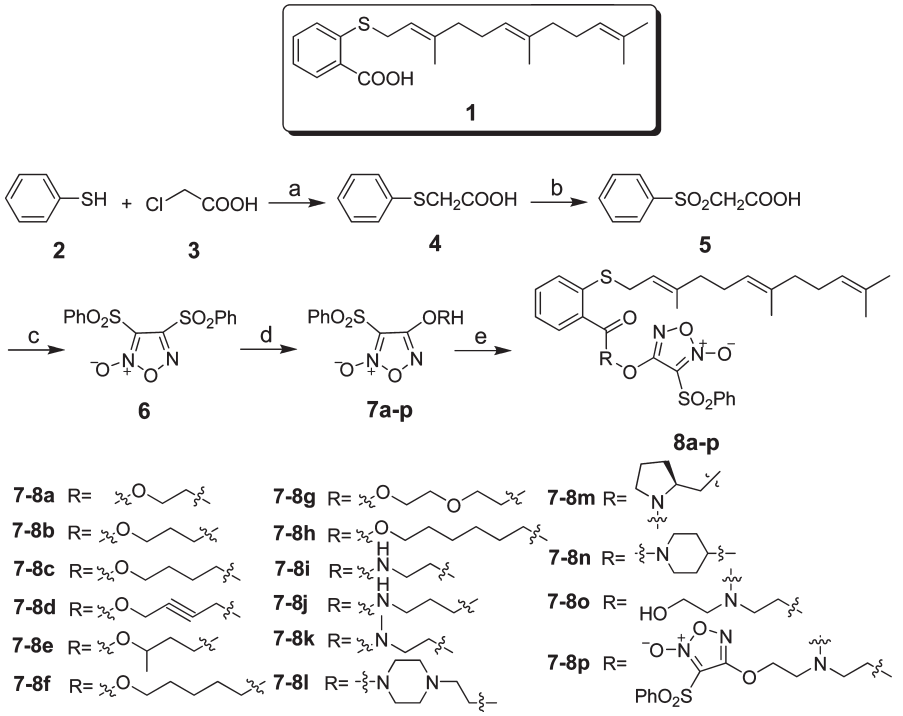

[a] Reagents and conditions: (a) $ClCH_2COOH$, NaOH(aq), 140 °C, 2 h. (b) 30% H_2O_2, AcOH, room temperature, 3 h. (c) Fuming HNO_3, 90 °C, 4 h. (d) Diol or alkanolamine, THF, 30% NaOH, room temperature, 4−8 h. (e) Compound **1**, DCC, DMAP, CH_2Cl_2, room temperature, 6−12 h.

potent cytotoxicity against HCC cells. Therefore, a total of 16 target compounds (**8a**−**p**) were designed and synthesized by coupling the carboxyl group of FTS with phenylsulfonyl-substituted furoxan through various diol or alkanolamine linkers. Their in vitro and in vivo anti-HCC activities, NO-releasing ability, acute toxicity, and inhibitory effect on the Ras-related signaling were evaluated. Herein, we report the synthesis and biological evaluation of these compounds.

RESULTS AND DISCUSSION

Chemistry. The substituted furoxans were prepared in a four-step sequence. The starting material benzenethiol (**2**) was converted to 2-(phenylthio)acetic acid (**4**) by treatment with chloroacetic acid (**3**). Compound **4** was oxidized by 30% H_2O_2 aqueous solution to give 2-(phenylsulfonyl) acetic acid (**5**) and reacted with fuming HNO_3 to form diphenylsulfonylfuroxan (**6**), which was then converted to various monophenylsulfonylfuroxans (**7a**−**p**) by treatment with corresponding diol or amino-substituted alcohol. Finally, the resulting furoxans were treated with *S-trans,trans*-FTS (**1**) to give the target compounds (**8a**−**p**), as shown in Scheme 1. The products **8a**−**p** were purified by column chromatography, and their structures were characterized by IR, ^1H NMR, MS, and elemental analyses. The purity of individual compounds was determined by high-performance liquid chromatography (HPLC, see the Supporting Information). Individual compounds with purity of >95% were used for subsequent experiments.

In Vitro Assessment. The effects of individual compounds on the proliferation of human HCC SMMC-7721, Bel7402, HepG2, and Hep3B cells was evaluated by MTT assay using FTS, **7l** (NO donor moiety), and sorafenib as positive controls. The IC_{50} values of individual compounds against each tumor cell line are presented in Table 1. Ten out of 16 compounds displayed inhibitory effects on the proliferation of HCC cells, which were superior to FTS, some even stronger than sorafenib or **7l**. For example, the inhibitory effects of **8i**, **8k**, **8l**, **8n**, and **8o** (IC_{50} = 5.35−12.20 μM) on the proliferation of Hep 3B cells were slightly stronger than that of sorafenib (IC_{50} = 14.08 μM), much stronger than that of FTS (IC_{50} = 63.75 μM). Notably, the IC_{50} of **8l** (1.36−5.35 μM) against four HCC cells was 3−8-fold less than those of sorafenib (IC_{50} = 10.26−17.30 μM), 4−15-fold less than that of **7l** (IC_{50} = 17.58−20.98 μM), and much less than that of FTS (IC_{50} = 63.75−107.51 μM), respectively. The strong inhibition of **8l** on the proliferation of these HCC cells may reflect the synergistic effect of high levels of NO and potent inhibition of the Ras-related signaling of the new hybrid.

Furthermore, we tested whether the strong inhibition of individual compounds on the proliferation of HCC cells could be associated with high levels of NO production in HepG2 cells. HepG2 and nontumor LO2 cells were exposed to each compound (100 μM) for varying durations (30−300 min). The levels of nitrite/nitrate produced in the lysates of these cells were characterized by the Griess assay (Figure 1). As expected, treatment with FTS resulted in little nitrite/nitrate in any of the tested cells. In contrast, treatment with individual furoxan/FTS hybrids promoted variable levels of nitrite/nitrate production in HepG2 cells. Treatment with low inhibitory **8d** and **8m** produced lower levels of nitrate/nitrite in these cells. However, treatment of compounds such as **8l** or **8o** with high inhibitory activity produced significantly higher levels of nitrate/nitrite in these cells. More importantly, the levels of nitrate/nitrite produced by those compounds were positively correlated with their inhibitions on the proliferation of HCC cells in vitro (R = 0.63,

dx.doi.org/10.1021/jm1014814 |*J. Med. Chem.* 2011, 54, 3251–3259

Table 1. IC_{50} Values of 8a−p against Four Human HCC Cell Lines

	in vitro inhibition of HCC proliferation (IC_{50}, μmol/L)[a]			
compd	Hep 3B	Hep G2	SMMC-7721	Bel-7402
FTS	63.75	107.51	71.22	76.13
sorafenib	14.08	11.49	17.30	10.26
7l	ND[b]	17.58	18.25	20.98
8a	>50	>50	>50	>50
8b	>50	>50	>50	>50
8c	>50	>50	>50	>50
8d	34.31	>50	37.14	35.82
8e	38.57	>50	43.71	>50
8f	>50	>50	>50	>50
8g	22.36	41.91	27.65	19.22
8h	>50	>50	>50	>50
8i	7.18	11.09	16.23	12.36
8j	18.83	29.15	19.74	21.99
8k	12.20	15.22	8.70	18.11
8l	5.35	1.36	4.72	4.48
8m	31.50	>50	34.97	21.14
8n	8.48	10.88	14.93	10.71
8o	10.35	13.70	14.56	8.60
8p	ND	ND	ND	ND

[a] The inhibitory effects of individual compounds on the proliferation of cancer cell lines were determined by the MTT assay and expressed as the IC_{50} (a dose achieved 50% inhibition in the proliferation of cancer cells cultured). [b] ND, not determined.

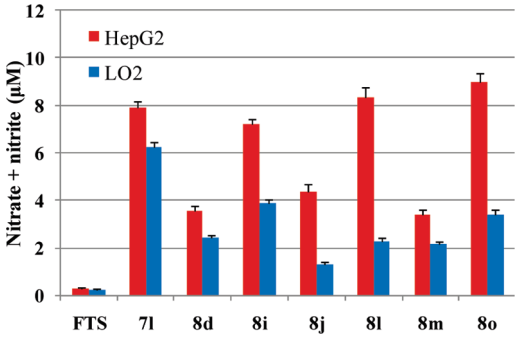

Figure 1. Variable levels of NO were produced by the compounds. HepG2 and LO2 cells were treated with each compound at 100 μM, and the contents of nitrate/nitrite in the cell lysates were determined by Griess assay through the duration of 30−300 min. The individual values were determined by measuring absorbance at 540 nm and calculated according to the standard curve. Data shown are the mean values ± SEMs of individual compounds at 240 min post-treatment in individual types of cells from three experiments, and similar patterns of nitrate/nitrite production in these cells were observed at other experimental time points (data not shown).

$p < 0.05$, determined by Pearson's correlation analysis). In addition, treatment with these compounds, particularly for those with strong inhibition, resulted in high levels of nitrite/nitrate production selectively in HepG2 cells. Evidently, the levels of nitrite/nitrate produced by **8l** or **8o** in HepG2 cells were much higher than that in LO2 cells. Therefore, some new compounds can produce high levels of NO selectively in HCC cells, which is

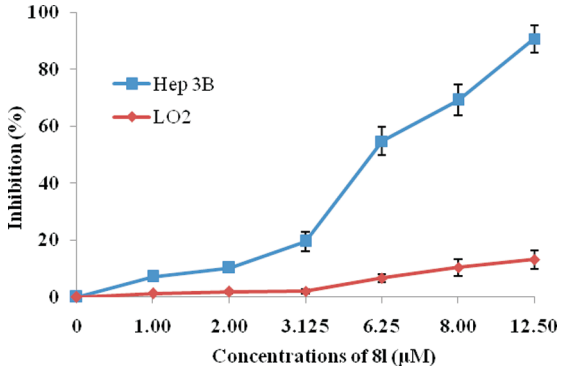

Figure 2. Inhibition of **8l** on the proliferation of Hep3B and LO2 cells. Hep3B and LO2 cells were treated with the indicated concentrations of **8l** for 48 h. The inhibitory effect on the proliferation of **8l** was determined by MTT assay. Data are expressed as means ± SEMs of inhibition (%) from three independent experiments.

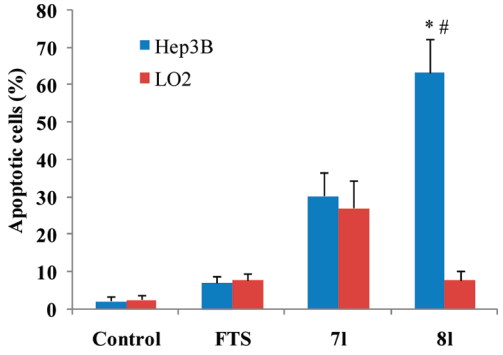

Figure 3. Compound **8l** selectively induces Hep3B cell apoptosis in vitro. Hep3B and LO2 cells were treated in duplicate with 8 μM **8l**, **7l**, FTS, or vehicle control for 48 h, respectively. The cells were harvested and stained with Annexin V and PI, followed by flow cytometry analysis. Data are expressed as means ± SEMs of each group of cells from three separate experiments. $^{*}p < 0.05$ vs LO2 cells; $^{\#}p < 0.05$ vs the other groups, respectively, determined by X^2 tests.

associated with their strong inhibition against HCC cell proliferation in vitro.

High levels of NO produced in HCC by these new furoxan/FTS compounds may result in selective inhibition on the proliferation of HCC and may even be cytotoxic to HCC. To test this hypothesis, we determined the inhibition of compound **8l** on the proliferation of Hep3B cells and nontumor liver LO2 cells in vitro. While treatment with 12.5 μM **8l** promoted nearly 90% of the inhibition in Hep3B cells, the same treatment only induced 10% of inhibition in LO2 cells, which was similar to that of unmanipulated cells in our experimental condition (data not shown, Figure 2). Apparently, **8l** has selective inhibition on the proliferation of HCC cells in vitro.

Given that FTS can sensitize tumor cells to apoptotic inducers and high levels of NO are cytotoxic to HCC cells, we further tested whether treatment with **8l** could selectively induce HCC cell apoptosis in vitro. Hep3B and nontumor LO2 cells were treated with 8 μM **8l**, **7l** (NO donor moiety of **8l**), FTS, or vehicle for 48 h, respectively. The cells were harvested and stained with Annexin V and propidium iodide (PI), and the percentages of apoptotic cells were determined by flow cytometry analysis (Figure 3). Treatment with FTS did not cause both

dx.doi.org/10.1021/jm1014814 |J. Med. Chem. 2011, 54, 3251–3259

Table 2. Acute Toxicity of 8l in Mice

		no. of dead mice								
dose (mg/kg)	no. of mice	1 h	4 h	1 day	2 days	3 days	4 days	5−14 days	total death	survival (%) on day 14
585.9	10	0	0	2	2	1	2	1	8	20
468.8	10	0	0	1	0	2	1	0	4	60
375.0	10	0	0	0	1	1	0	0	2	80
300.0	10	0	0	0	0	1	0	0	1	90
240.0	10	0	0	0	0	0	0	0	0	100
vehicle	10	0	0	0	0	0	0	0	0	100

Hep3B and LO2 cell apoptosis as the percentages of apoptotic Hep3B and LO2 cells were similar to those of the cells treated with vehicle. Furthermore, treatment with **7l** induced moderate frequency of Hep3B cell apoptosis, whereas treatment with **8l** triggered nearly 65% of Hep3B cell apoptosis. More importantly, treatment with **8l** did not cause nontumor LO2 cell apoptosis. These data indicated that the new furoxan/FTS hybrid **8l** selectively induced high frequency of HCC cell apoptosis.

In Vivo Anti-HCC Activity of 8l. To evaluate the safety of **8l**, groups of female KM mice were injected intraperitoneally with a single dose of **8l** at 585.9, 468.8, 375.0, 300.0, and 240.0 mg/kg or vehicle control, respectively, according to our pilot study. The survival of mice was monitored up to 14 days postinjection (Table 2). Treatment with **8l** at a high dose (585.9 mg/kg) killed almost all mice, and the LD_{50} value of **8l** is 467.1 mg/kg for this strain of mice. In contrast, injection with **8l** at 240.0 mg/kg, like with vehicle alone, did not cause any abnormality in the mice throughout the observation period, suggesting injection with **8l** at or below this dose may be safe for mice.

To evaluate the in vivo activity of **8l**, BALB/c nude mice were inoculated subcutaneously with SMMC7721 cells. After the establishment of solid tumor, the mice were randomized and treated with 15 or 60 mg/kg of **8l**, positive control FTS (16 mg/kg), or vehicle alone, respectively. Treatment with vehicle alone did not change the growth of tumors in vivo because the dynamic increases in the volumes of HCC tumors in the vehicle-treated mice were similar to those in untreated controls (data not shown). In contrast, treatment with **8l** at 15 mg/kg significantly inhibited the growth of HCC tumor ($p < 0.01$ vs. controls). Treatment with 60 mg/kg of **8l** enhanced the inhibitory effect on the growth of HCC tumors ($p < 0.01$ vs treatment with 15 mg/kg), and its inhibitory effect was slightly stronger than that of FTS treatment (Figure 4). Importantly, the tumor weights in the mice treated with **8l** at 15 or 60 mg/kg were 0.98 ± 0.19 or 0.72 ± 0.33 g, respectively, which were significantly less than those from the vehicle-treated controls (1.53 ± 0.71 g, $p < 0.01$). Together, our data clearly demonstrate that **8l** is a relatively safe reagent and can inhibit the growth of HCC in vivo.

Effect of 8l on the Ras-Related Signaling. Finally, we examined the effect of treatment with **8l** on the Ras-related signaling in vivo. The expression and phosphorylation levels of the Ras-related signal events, Akt, extracellular signal-regulated kinase (ERK), and c-Raf in the homogenates of liver tumors dissected from the mice that had been treated with FTS, vehicle control, and 15 or 60 mg/kg of **8l** were determined by immunoblotting assays. Treatment with FTS inhibited the phosphorylation of c-Raf, Akt, and ERK, while treatment with **8l** further down-regulated the phosphorylation levels of these events in the liver tumor (Figure 5A). Quantitative analysis revealed that

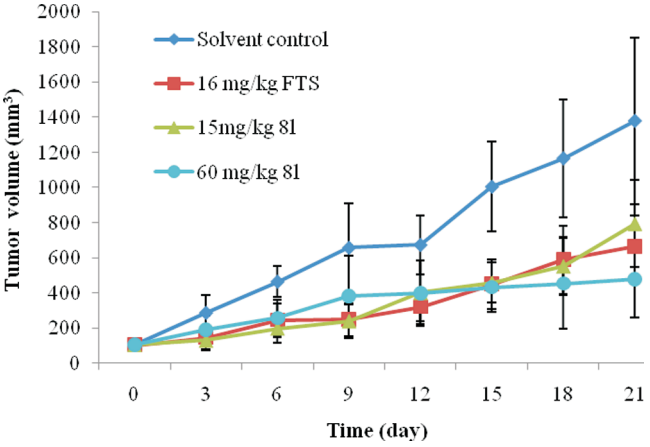

Figure 4. Effect of **8l** on the growth of HCC tumors in vivo. BALB/c nude mice were inoculated with SMMC7721 cells. After establishment of solid tumor, the mice were randomized and treated with solvent control, FTS, or **8l** at the indicated doses, respectively, and the growth of tumors was measured longitudinally. Data are expressed as means ± SEMs of tumor volumes at each time point for each group of mice ($n = 6$ per group). The kinetics of HCC tumor growth in untreated controls was similar to that of solvent controls (data not shown).

similar levels of Akt expression were detected in these groups of liver tumors, and the relative levels of Akt phosphorylation in the FTS-treated tumors were significantly lower than those in control tumors (Figure 5B). The levels of Akt phosphorylation in the **8l**-treated tumors were further reduced significantly, as compared with those in the FTS-treated tumors. Furthermore, similar patterns of the inhibition of c-Raf and ERK phosphorylation by **8l** were observed although treatment with either compound significantly down-regulated the expression of ERK in these groups of liver tumors. These data clearly indicated that treatment with **8l** inhibited the ERK expression and the c-Raf, Akt, and ERK phosphorylation in the liver tumors, which may contribute to the inhibition of tumor growth in vivo. The significantly higher inhibition of **8l** on the Ras-related signaling suggests that high levels of NO produced by **8l** may enhance the inhibition of FTS on the Ras-related signaling in the liver tumors.

Structure−Activity Relationships (SARs). Analysis of SAR revealed that **8a−p** with different linkers displayed variable inhibitory effects on the proliferation of HCC cells. The compounds (**8i−o**) linked with alkanolamine exhibited stronger inhibitory effects than the compounds (**8a−h**) linked with diol. The different pharmacological profile of these compounds may be attributed to the fact that the linkers modulate the structure, stability, metabolism, penetrability, and activity of these

dx.doi.org/10.1021/jm1014814 |J. Med. Chem. 2011, 54, 3251–3259

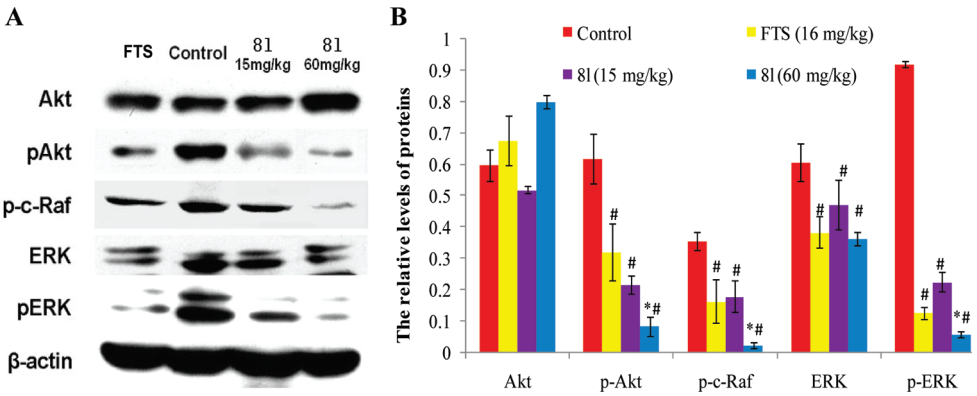

Figure 5. Immunoblot analysis of the expression and phosphorylation of Akt, ERK, and c-Raf in the tumors. Individual liver tumors from the mice that had been treated with vehicle (control), FTS, or different doses of **8l** were homogenized, and their lysates were subjected to immunoblot analysis using anti-Akt, antiphospho-Akt (Ser473), anti-ERK, antiphospho-ERK (Thr202/Tyr204), antiphospho-c-Raf (Ser259), and anti-β-actin antibodies, respectively. (A) A representative blot. Data shown are a representative image from six separate experiments. (B) Quantitative analysis. The relative levels of each signaling event to control β-actin were determined by densimetric scanning. Data are expressed as means ± SDs of each protein of each group (n = 6 per group) from six separate experiments. $^{\#}p < 0.05$ vs control; $^{*}p < 0.05$ vs FTS, determined by Student's t test.

compounds in HCC. It is likely that the ester compounds can usually be metabolized into the corresponding acid and alcohol, which may lead to the partial loss of their inhibitory activity. Indeed, the ester derivatives of FTS such as **8a**−**c** displayed the lowest activity against HCC cells. In sharp contrast, the amide derivatives of FTS such as **8l** had the strongest inhibitory activity among the compounds tested. The higher inhibitory activity of **8l** may come from higher levels of NO release and stronger inhibition of the Ras-related signaling in comparison with the ester derivatives. Furthermore, among the amide derivatives of FTS, compounds **8i**, **8k**, and **8o** with an aminoethanol linker had higher inhibition on the proliferation of HCC cells than those with an aminopropanol linker, like **8j**. The different activity of those compounds may stem from the variable metabolic pathways since it is known that the aminoethanol can be oxidized and contribute to the formation of glycine, and the aminopropanol is usually metabolized rapidly by aminopropanol-dehydrogenase in the liver.[29,30] Strikingly, the compound **8m** with a pyrrolidinylmethanol linker displayed the lowest inhibition on the proliferation of HCC cells. However, the precise mechanisms underlying the SAR of these furoxan/FTS hybrids remain further investigation.

CONCLUSIONS

In summary, most novel furoxan-based NO-releasing derivatives of FTS displayed a strong inhibition on the proliferation of HCC cells in vitro, particularly for **8l**, which had a great potency superior to sorafenib, produced high levels of NO in HCC cells, and induced high frequency of HCC cell apoptosis in vitro. Interestingly, the cytotoxicity of **8l** appeared to be selectively against HCC. Evidentially, **8l** exhibited very weak activity against human nontumor liver LO2 cells and produced low levels of NO in LO2 cells. The low cytotoxicity of **8l** against nontumor cells, together with low acute toxicity in mice, suggests that **8l** may be a relative safe anti-HCC agent. More importantly, treatment with **8l** inhibited the growth of HCC tumors and the Ras-related signaling in vivo. Apparently, the synergic effect of high levels of NO production and strong inhibition on the Ras-related signaling contributed to its potent cytotoxicity against HCC. Accordingly, **8l** may be a promising candidate for further intensive study. Therefore, our novel findings may provide a new framework for the design of new NO-releasing furoxan/FTS hybrids for the intervention of human HCC.

EXPERIMENTAL SECTION

Melting points of individual compounds were determined on a Mel-TEMP II melting point apparatus and uncorrected. Optical rotations were measured with a JASCO P-1020 polarimeter (cell length, 100 mm). Infrared (IR) spectra (KBr) were recorded on a Nicolet Impact 410 instrument (KBr pellet). ^{1}H NMR spectra were recorded with a Bruker Avance 300 MHz spectrometer at 300 K, using TMS as an internal standard. MS spectra were recorded on a Shimadzu GC-MS 2010 (EI) or a Mariner Mass Spectrum (ESI). Element analysis was performed on an Eager 300 instrument. All compounds were routinely checked by TLC and ^{1}H NMR. TLCs and preparative TLC were performed on silica gel GF/UV 254, and the chromatograms were conducted on silica gel (200−300 mesh) and visualized under UV light at 254 and 365 nm. All solvents were reagent grade and, when necessary, were purified and dried by standards methods. Solutions after reactions and extractions were concentrated using a rotary evaporator operating at a reduced pressure of ca. 20 Torr. Organic solutions were dried over anhydrous sodium sulfate. Compounds **1**−**3** were commercially available. Compounds **4**−**6** and **7a**−**i** were synthesized, as previously described.[24]

General Procedure for the Preparation of 7j−**p.** Compound **6** (1.0 g, 2.7 mmol) in 15 mL of THF was mixed with corresponding alkanolamine (10.9 mmol) by stirring at 0 °C, followed by reaction with 1 mL of 15% NaOH at room temperature for 4−12 h with stirring. The mixture was concentrated in vacuo, dissolved in 15 mL of H_2O, and extracted with CH_2Cl_2 (10 mL × 3). The organic layer was combined, washed with water and saturated NaCl solution sequentially, dried over anhydrous Na_2SO_4, and concentrated in vacuo. The crude product was purified by column chromatography (EtOAc to MeOH/CH_2Cl_2 1:8 v/v) to give the title compounds (50−88%).

4-(3-Aminopropoxy)-3-(phenylsulfonyl)-1,2,5-oxadiazole-2-oxide (7j). The title compound was obtained starting from **6** and propanolamine. White waxy solid, 70% yield. Analytical data for **7j**: ^{1}H NMR ($CDCl_3$, 300 MHz): δ 8.05 (m, 2H, Ar−H), 7.75 (m, 1H, Ar−H), 7.61 (m, 2H, Ar−H), 4.54 (t, 2H, J = 6.0 Hz, OCH_2), 2.96 (t, 2H, J = 6.6 Hz, NCH_2), 2.03 (m, 4H, $NCH_2\underline{CH_2}$, NH_2). MS (ESI) m/z = 300 $[M + 1]^+$. Anal. calcd for $C_{11}H_{13}N_3O_5S$: C, 44.14; H, 4.38; N, 14.04. Found: C, 43.87; H, 4.60; N, 13.91.

dx.doi.org/10.1021/jm1014814 |J. Med. Chem. 2011, 54, 3251–3259

4-(2-(Methylamino)ethoxy)-3-(phenylsulfonyl)-1,2,5-oxadiazole-2-oxide (7k). The title compound was obtained starting from **6** and 2-(methylamino)ethanol. Yellow cream, 50% yield. This product was unstable and was used for the next step without any further purification.

3-(Phenylsulfonyl)-4-(2-(piperazin-1-yl)ethoxy)-1,2,5-oxadiazole-2-oxide (7l). The title compound was obtained starting from **6** and 2-(piperazin-1-yl)ethanol. Pale yellow waxy solid, 56% yield. Analytical data for **7l**: ^{1}H NMR ($CDCl_3$, 300 MHz): δ 8.06 (d, 2H, J = 7.5 Hz, Ar−H), 7.78 (m 1H, Ar−H), 7.64 (m, 2H, Ar−H), 4.56 (t, 2H, J = 5.7 Hz, CH_2O), 2.94 (m, 6H, $HN(CH_2)_2$, NCH_2), 2.64 (m, 4H, $(CH_2)_2N$), 1.99 (m, 1H, NH); MS (ESI) m/z = 355 $[M + 1]^+$. Anal. calcd for $C_{14}H_{18}N_4O_5S$: C, 47.45; H, 5.12; N, 15.81. Found: C, 47.22; H, 5.38; N, 15.66.

(*S*)-3-(Phenylsulfonyl)-4-(pyrrolidin-2-ylmethoxy)-1,2,5-oxadiazole-2-oxide (7m). The title compound was obtained starting from **6** and (*S*)-pyrrolidin-2-ylmethanol. Pale yellow waxy solid, 88% yield. Analytical data for **7m**: $[\alpha]_D^{24}$: −2.36. ^{1}H NMR ($CDCl_3$, 300 MHz): δ 8.07 (d, 2H, J = 7.8 Hz, Ar−H), 7.75 (m, 1H, Ar−H), 7.61 (m, 2H, Ar−H), 4.31(m, 2H, OCH_2), 3.69 (m, 1H, NCH), 3.07 (m, 2H, NCH_2), 2.02 (m, 1H, NH), 1.91 (m, 4H, $CHCH_2CH_2$). MS (ESI) m/z = 326 $[M + 1]^+$. Anal. calcd for $C_{13}H_{15}N_3O_5S$: C, 47.99; H, 4.65; N, 12.92. Found: C, 47.83; H, 4.99; N, 12.53.

3-(Phenylsulfonyl)-4-(piperidin-4-yloxy)-1,2,5-oxadiazole-2-oxide (7n). The title compound was obtained starting from **6** and piperidin-4-ol. White solid, mp 78−81 °C, 61% yield. Analytical data for **7n**: ^{1}H NMR ($CDCl_3$, 300 MHz): δ 8.05 (m, 2H, Ar−H), 7.77 (m, 1H, Ar−H), 7.66 (m, 2H, Ar−H), 5.05 (m, 1H, OCH), 3.00 (m, 4H, $N(CH_2)_2$), 1.90 (m, 5H, $C(CH_2)_2$, NH). MS (ESI) m/z = 326 $[M + 1]^+$. Anal. calcd for $C_{13}H_{15}N_3O_5S$: C, 47.99; H, 4.65; N, 12.92. Found: C, 48.26; H, 4.52; N, 12.97.

4-(2-(2-Hydroxyethylamino)ethoxy)-3-(phenylsulfonyl)-1,2,5-oxadiazole-2-oxide (7o). These two compounds were obtained starting from **6** and diethanolamine. Pale yellow waxy solid, 65% yield. Analytical data for **7o**: ^{1}H NMR ($CDCl_3$, 300 MHz): δ 8.05 (d, 2H, J = 7.5 Hz, Ar−H), 7.77 (m, 1H, Ar−H), 7.63 (m, 2H, Ar−H), 4.55 (m, 2H, OCH_2), 4.12 (m, 1H, OH), 3.84 (m, 2H, $HOCH_2$), 3.15 (m, 2H, NCH_2), 2.92 (t, 2H, J = 5.1 Hz, $HOCH_2CH_2$), 2.27 (m, 1H, NH). MS (ESI) m/z = 330 $[M + 1]^+$. Anal. calcd for $C_{12}H_{15}N_3O_6S$: C, 43.76; H, 4.59; N, 12.76. Found: C, 43.29; H, 4.55; N, 12.72.

4,4′-(2,2′-Azanediylbis(ethane-2,1-diyl)bis(oxy))bis(3-(phenylsulfonyl)-1,2,5-oxadiazole-2-oxide) (7p). The title compound was obtained starting from **6** and diethanolamine. Pale yellow waxy solid, 8% yield. Analytical data for **7p**: ^{1}H NMR ($CDCl_3$, 300 MHz): δ 8.07 (d, 4H, J = 8.1 Hz, Ar−H), 7.74 (m, 2H, Ar−H), 7.60 (m, 2H, Ar−H), 7.31 (m, 2H, Ar−H), 4.62 (m, 4H, 2 × OCH_2), 3.52 (m, 4H, 2 × NCH_2). MS (ESI) m/z = 554 $[M + 1]^+$. Anal. calcd for $C_{20}H_{19}N_5O_{10}S_2$: C, 43.40; H, 3.46; N, 12.65. Found: C, 43.16; H, 3.71; N, 12.49.

General Procedure for the Preparation of 8a−p. To a solution of **1** (400 mg, 1.12 mmol) in dry CH_2Cl_2 (40 mL), **7a−p** (1.23 mmol), dicyclohexylcarbodiimide (DCC) (270 mg, 1.34 mmol), and 4-dimethylaminopyridine (DMAP) (100 mg, 0.82 mmol) was added, and the mixture was stirred at room temperature for 6−12 h. After filtration, the filtrate was evaporated to dryness in vacuo, and the crude product was purified by column chromatography [petroleum ether (PE)/EtOAc = 6:1 to 3:1 v/v] to yield **8a−p** (46−70%).

3-(Phenylsulfonyl)-4-(2-(2-((2*E*,6*E*)-3,7,11-trimethyldodeca-2,6,10-trienylthio)benzoyloxy)ethyloxy)-1,2,5-oxadiazole-2-oxide (8a). The title compound was obtained starting from **1** and **7a**. Colorless viscous liquid, 61% yield. Analytical data for **8a**: IR (KBr, cm^{-1}): 3418, 2925, 1715, 1613, 1452, 1171. ^{1}H NMR ($CDCl_3$, 300 MHz): δ 8.03 (m, 2H, Ar−H), 7.91 (m, 1H, Ar−H), 7.70 (t, 1H, J = 7.5 Hz, Ar−H), 7.60 (m, 2H, Ar−H), 7.41 (m, 1H, Ar−H), 7.25 (m, 1H, Ar−H), 7.12 (m, 1H, Ar−H), 5.31 (m, 1H, SCH_2CH), 5.05 (t, 2H, J = 7.2 Hz, 2 × CH_2CH=CCH_3), 4.58 (t, 2H, J = 6.0 Hz, $COOCH_2$), 4.50 (t, 2H, J = 6.0 Hz, OCH_2), 3.54 (d, 2H, J = 7.5 Hz, SCH_2), 1.87−2.00 (m, 8H, 2 × $CHCH_2CH_2CH$), 1.55−1.68 (m, 12H, 4 × CH=CCH_3). MS (ESI) m/z = 627 $[M + 1]^+$. Anal. calcd for $C_{32}H_{38}N_2O_7S_2$: C, 61.32; H, 6.11; N, 4.47. Found: C, 61.55; H, 5.87; N, 4.30.

3-(Phenylsulfonyl)-4-(3-(2-((2*E*,6*E*)-3,7,11-trimethyldodeca-2,6,10-trienylthio)benzoyloxy)propoxy)-1,2,5-oxadiazole-2-oxide (8b). The title compound was obtained starting from **1** and **7b**. Colorless viscous liquid, 70% yield. Analytical data for **8b**: IR (KBr, cm^{-1}): 3422, 2965, 1712, 1615, 1553, 1450, 1248, 1170. ^{1}H NMR ($CDCl_3$, 300 MHz): δ 8.05 (m, 2H, Ar−H), 7.94 (m, 1H, Ar−H), 7.73 (t, 1H, J = 7.5 Hz, Ar−H), 7.62 (m, 2H, Ar−H), 7.44 (m, 1H, Ar−H), 7.28 (m, 1H, Ar−H), 7.15 (m, 1H, Ar−H), 5.33 (m, 1H, SCH_2CH), 5.08 (m, 2H, 2 × CH_2CH=CCH_3), 4.61 (t, 2H, J = 6.0 Hz, $COOCH_2$), 4.51 (t, 2H, J = 6.0 Hz, OCH_2), 3.57 (d, 2H, J = 7.5 Hz, SCH_2), 2.36 (m, 2H, $CH_2CH_2CH_2$), 1.89−2.02 (m, 8H, 2 × $CHCH_2CH_2CH$), 1.50−1.68 (m, 12H, 4 × CH=CCH_3). MS (ESI) m/z = 641 $[M + 1]^+$. Anal. calcd for $C_{33}H_{40}N_2O_7S_2$: C, 61.85; H, 6.29; N, 4.37. Found: C, 61.62; H, 6.08; N, 4.22.

3-(Phenylsulfonyl)-4-(4-(2-((2*E*,6*E*)-3,7,11-trimethyldodeca-2,6,10-trienylthio)benzoyloxy)butoxy)-1,2,5-oxadiazole-2-oxide (8c). The title compound was obtained starting from **1** and **7c**. Colorless viscous liquid, 64% yield. Analytical data for **8c**: IR (KBr, cm^{-1}): 3408, 2931, 1709, 1462, 1281, 1058. ^{1}H NMR ($CDCl_3$, 300 MHz): δ 7.95 (m, 2H, Ar−H), 7.43 (m, 2H, Ar−H), 7.42 (t, 2H, J = 7.5 Hz, Ar−H), 7.29 (m, 2H, Ar−H), 7.14 (m, 1H, Ar−H), 5.33 (m, 1H, SCH_2CH), 5.06 (m, 2H, 2 × CH_2CH=CCH_3), 4.35 (t, 2H, J = 6.9 Hz, $COOCH_2$), 3.70 (t, 2H, J = 6.0 Hz, OCH_2), 3.57 (m, 2H, SCH_2), 1.83−2.02 (m, 12H, 2 × $CHCH_2CH_2CH$, $CH_2CH_2CH_2CH_2$), 1.50−1.68 (m, 12H, 4 × CH=CCH_3). MS (ESI) m/z = 655 $[M + 1]^+$. Anal. calcd for $C_{34}H_{42}N_2O_7S_2$: C, 62.36; H, 6.46; N, 4.28. Found: C, 62.23; H, 6.60; N, 4.27.

3-(Phenylsulfonyl)-4-(4-(2-((2*E*,6*E*)-3,7,11-trimethyldodeca-2,6,10-trienylthio)benzoyloxy)but-2-ynyloxy)-1,2,5-oxadiazole-2-oxide (8d). The title compound was obtained starting from **1** and **7d**. Colorless viscous liquid, 61% yield. Analytical data for **8d**: IR (KBr, cm^{-1}): 3327, 2928, 1718, 1624, 1450, 1243, 1056. ^{1}H NMR ($CDCl_3$, 300 MHz): δ 8.06 (d, 2H, J = 7.8 Hz, Ar−H), 8.01 (d, 1H, J = 7.8 Hz, Ar−H), 7.74 (t, 1H, J = 7.2 Hz, Ar−H), 7.62 (m, 2H, Ar−H), 7.47 (t, 1H, Ar−H), 7.33 (m, 1H, Ar−H), 7.20 (m, 1H, Ar−H), 5.33 (m, 1H, SCH_2CH), 5.12 (m, 4H, 2 × CH_2CH=CCH_3, $COOCH_2$), 5.00 (s, 2H, OCH_2), 3.60 (d, 2H, J = 7.2 Hz, SCH_2), 1.88−2.04 (m, 8H, 2 × $CHCH_2CH_2CH$), 1.48−1.68 (m, 12H, 4 × CH=CCH_3). MS (ESI) m/z = 651 $[M + 1]^+$. Anal. calcd for $C_{34}H_{38}N_2O_7S_2$: C, 62.75; H, 5.89; N, 4.30. Found: C, 62.48; H, 6.11; N, 4.13.

3-(Phenylsulfonyl)-4-(3-(2-((2*E*,6*E*)-3,7,11-trimethyldodeca-2,6,10-trienylthio)benzoyloxy)butoxy)-1,2,5-oxadiazole 2-oxide (8e). The title compound was obtained starting from **1** and **7e**. Colorless viscous liquid, 57% yield. Analytical data for **8e**: IR (KBr, cm^{-1}): 3441, 2925, 1708, 1615, 1450, 1248, 1170, 1057. ^{1}H NMR ($CDCl_3$, 300 MHz): δ 8.08 (d, 2H, J = 7.8 Hz, Ar−H), 7.93 (d, 1H, J = 7.5 Hz, Ar−H), 7.73 (m, 1H, Ar−H), 7.64 (m, 2H, Ar−H), 7.43 (t, 1H, J = 7.2 Hz, Ar−H), 7.30 (m, 1H, Ar−H), 7.16 (m, 1H, Ar−H), 5.40 (m, 1H, SCH_2CH), 5.08 (m, 2H, 2 × CH_2CH=CCH_3), 4.56 (t, 2H, J = 6.0 Hz, OCH_2), 4.31 (m, 1H, OCH), 3.56 (d, 2H, J = 7.2 Hz, SCH_2), 2.28 (m, 2H, $CHCH_2$), 1.89−2.02 (m, 8H, 2 × $CHCH_2CH_2CH$), 1.50−1.68 (m, 12H, 4 × CH=CCH_3), 1.47 (d, 3H, J = 6.3 Hz, $CHCH_3$). MS (ESI) m/z = 655 $[M + 1]^+$. Anal. calcd for $C_{34}H_{42}N_2O_7S_2$: C, 62.36; H, 6.46; N, 4.28. Found: C, 62.11; H, 6.85; N, 4.38.

3-(Phenylsulfonyl)-4-(5-(2-((2*E*,6*E*)-3,7,11-trimethyldodeca-2,6,10-trienylthio)benzoyloxy)pentyloxy)-1,2,5-oxadiazole-2-oxide (8f). The title compound was obtained starting from **1**

and **7f**. Colorless viscous liquid, 68% yield. Analytical data for **8f**: IR (KBr, cm^{-1}): 3441, 2925, 1710, 1615, 1552, 1450, 1248, 1170. ^1H NMR ($CDCl_3$, 300 MHz): δ 8.04 (d, 2H, J = 7.5 Hz, Ar−H), 7.96 (d, 1H, J = 7.8 Hz, Ar−H), 7.73 (m, 1H, Ar−H), 7.59 (m, 2H, Ar−H), 7.42 (m, 1H, Ar−H), 7.32 (m, 1H, Ar−H), 7.14 (m, 1H, Ar−H), 5.34 (m, 1H, SCH_2CH), 5.09 (m, 2H, 2 × CH_2CH=CCH_3), 4.44 (t, 2H, J = 6.3 Hz, $COOCH_2$), 4.37 (t, 2H, J = 6.6 Hz, OCH_2), 3.58 (d, 2H, J = 7.8 Hz, SCH_2), 1.89−2.02 (m, 8H, 2 × $CHCH_2CH_2CH$), 1.50−1.70 (m, 18H, 4 × CH=CCH_3, $CH_2CH_2CH_2CH_2CH_2$). MS (ESI) m/z = 669 $[M + 1]^+$. Anal. calcd for $C_{35}H_{44}N_2O_7S_2 \cdot 5.5H_2O$: C, 54.74; H, 7.22; N, 3.65. Found: C, 54.66; H, 6.92; N, 3.60.

3-(Phenylsulfonyl)-4-(2-(2-(2-((2*E*,6*E*)-3,7,11-trimethyldodeca-2,6,10-trienylthio)benzoyloxy)ethoxy) ethoxy)-1,2,5-oxadiazole-2-oxide (8g). The title compound was obtained starting from **1** and **7g**. Colorless viscous liquid, 67% yield. Analytical data for **8g**: IR (KBr, cm^{-1}): 3451, 2924, 1712, 1617, 1449, 1249, 1170. ^1H NMR ($CDCl_3$, 300 MHz): δ 7.96 (d, 1H, J = 7.8 Hz, Ar−H), 7.91 (d, 2H, J = 7.2 Hz, Ar−H), 7.62 (t, 1H, J = 7.5 Hz, Ar−H), 7.49 (m, 2H, Ar−H), 7.30 (m, 2H, Ar−H), 7.16 (m, 1H, Ar−H), 5.33 (m, 3H, SCH_2CH,2 × CH_2CH=CCH_3), 4.37 (m, 4H, 2 × CH_2O), 3.73 (m, 4H, CH_2OCH_2), 3.58 (d, 2H, J = 7.2 Hz, SCH_2), 1.89−2.02 (m, 8H, 2 × $CHCH_2CH_2CH$), 1.50−1.68 (m, 12H, 4 × CH=CCH_3). MS (ESI) m/z = 671 $[M + 1]^+$. Anal. calcd for $C_{34}H_{42}N_2O_8S_2$: C, 60.87; H, 6.31; N, 4.18. Found: C, 60.59; H, 6.52; N, 3.97.

3-(Phenylsulfonyl)-4-(6-(2-((2*E*,6*E*)-3,7,11-trimethyldodeca-2,6,10-trienylthio)benzoyloxy)hexyloxy)-1,2,5-oxadiazole-2-oxide (8h). The title compound was obtained starting from **1** and **7g**. Colorless viscous liquid, 65% yield. Analytical data for **8g**: IR (KBr, cm^{-1}): 3420, 2930, 1710, 1615, 1450, 1248, 1170. ^1H NMR ($CDCl_3$, 300 MHz): δ 8.04 (m, 2H, Ar−H), 7.95 (m, 1H, Ar−H), 7.75 (t, 1H, J = 7.5 Hz, Ar−H), 7.61 (m, 2H, Ar−H), 7.43 (m, 1H, Ar−H), 7.30 (m, 1H, Ar−H), 7.15 (m, 1H, Ar−H), 5.34 (m, 1H, SCH_2CH), 5.08 (m, 2H, 2 × CH_2CH=CCH_3), 4.42 (t, 2H, J = 6.3 Hz, $COOCH_2$), 4.34 (t, 2H, J = 6.6 Hz, OCH_2), 3.57 (d, 2H, J = 7.5 Hz, SCH_2), 1.89−2.02 (m, 8H, 2 × $CHCH_2CH_2CH$), 1.50−1.68 (m, 16H, 4 × CH=CCH_3, $COOCH_2CH_2$, CH_2CH_2O), 1.25 (m, 4H, OCH_2CH_2-CH_2CH_2). MS (ESI) m/z = 683 $[M + 1]^+$. Anal. calcd for $C_{36}H_{46}N_2O_7S_2$: C, 63.32; H, 6.79; N, 4.10. Found: C, 63.06; H, 6.98; N, 3.80.

3-(Phenylsulfonyl)-4-(2-(2-((2*E*,6*E*)-3,7,11-trimethyldodeca-2,6,10-trienylthio)benzamido)ethyloxy)-1,2,5-oxadiazole-2-oxide (8i). The title compound was obtained starting from **1** and **7i**. Colorless viscous liquid, 67% yield. Analytical data for **8i**: IR (KBr, cm^{-1}): 3333, 2928, 1621, 1554, 1453, 1260, 1167, 1021. ^1H NMR ($CDCl_3$, 300 MHz): δ 8.02 (d, 2H, J = 7.8 Hz, Ar−H), 7.70 (m, 2H, Ar−H), 7.55 (t, 2H, J = 7.8 Hz, Ar−H), 7.36 (m, 2H, Ar−H), 7.18 (m, 1H, Ar−H), 5.25 (m, 1H, SCH_2CH), 5.08 (m, 2H, 2 × CH_2CH=CCH_3), 4.64 (t, 2H, J = 4.8 Hz, CH_2O), 3.96 (m, 2H, NCH_2), 3.53 (d, 2H, J = 7.2 Hz, SCH_2), 1.89−2.02 (m, 8H, 2 × $CHCH_2CH_2CH$), 1.50−1.68 (m, 12H, 4 × CH=CCH_3). MS (ESI) m/z = 626 $[M + 1]^+$. Anal. calcd for $C_{32}H_{39}N_3O_6S_2 \cdot 0.2H_2O$: C, 61.06; H, 6.31; N, 6.68. Found: C, 61.22; H, 6.78; N, 6.23.

3-(Phenylsulfonyl)-4-(3-(2-((2*E*,6*E*)-3,7,11-trimethyldodeca-2,6,10-trienylthio)benzamido)propoxy)-1,2,5-oxadiazole-2-oxide (8j). The title compound was obtained starting from **1** and **7j**. Colorless viscous liquid, 67% yield. Analytical data for **8j**: IR (KBr, cm^{-1}): 3444, 1630, 1552, 1449, 1168, 1068. ^1H NMR ($CDCl_3$, 300 MHz): δ 8.00 (d, 2H, J = 7.5 Hz, Ar−H), 7.74 (t, 1H, J = 7.5 Hz, Ar−H), 7.61 (m, 3H, Ar−H), 7.40 (m, 2H, Ar−H), 7.30 (m, 1H, Ar−H), 5.26 (m, 1H, SCH_2CH), 5.07 (m, 2H, 2 × CH_2CH=CCH_3), 4.59 (t, 2H, J = 6.0 Hz, OCH_2), 3.71 (d, 2H, J = 7.8 Hz, SCH_2), 3.55 (d, 2H, J = 7.5 Hz, NCH_2), 2.26 (m, 2H, NCH_2CH_2), 1.89−2.02 (m, 8H, 2 × $CHCH_2CH_2CH$), 1.50−1.68 (m, 12H, 4 × CH=CCH_3). MS (ESI) m/z = 640 $[M + 1]^+$. Anal. calcd for $C_{33}H_{41}N_3O_6S_2$: C, 61.95; H, 6.46; N, 6.57. Found: C, 61.70; H, 6.70; N, 6.30.

4-(2-(*N*-Methyl-2-((2*E*,6*E*)-3,7,11-trimethyldodeca-2,6,10-trienylthio)benzamido)ethoxy)-3-(phenylsulfonyl)-1,2,5-oxadiazole-2-oxide (8k). The title compound was obtained starting from **1** and **7k**. Colorless viscous liquid, 60% yield. Analytical data for **8k**: IR (KBr, cm^{-1}): 3281, 2925, 1627, 1552, 1448, 1372, 1157. ^1H NMR ($CDCl_3$, 300 MHz): δ 8.07 (d, 2H, J = 7.5 Hz, Ar−H), 7.94 (m, 1H, Ar−H), 7.76 (m, 1H, Ar−H), 7.59 (m, 3H, Ar−H), 7.31 (m, 2H, Ar−H), 5.30 (m, 1H, SCH_2CH), 5.07 (m, 2H, 2 × CH_2CH=CCH_3), 4.77 (m, 2H, OCH_2), 4.06 (d, 2H, J = 7.8 Hz, SCH_2), 3.53 (m, 2H, NCH_2), 3.02 (m, 3H, NCH_3), 1.89−2.02 (m, 8H, 2 × $CHCH_2CH_2CH$), 1.50−1.68 (m, 12H, 4 × CH=CCH_3). MS (ESI) m/z = 640 $[M + 1]^+$. Anal. calcd for $C_{33}H_{41}N_3O_6S_2 \cdot 1.5H_2O$: C, 59.44; H, 6.55; N, 6.30. Found: C, 59.61; H, 6.19; N, 6.23.

3-(Phenylsulfonyl)-4-(2-(4-(2-((2*E*,6*E*)-3,7,11-trimethyldodeca-2,6,10-trienylthio)benzoyl)piperazin-1-yl)ethoxy)-1,2,5-oxadiazole-2-oxide (8l). The title compound was obtained starting from **1** and **7l**. Colorless viscous liquid, 63% yield. Analytical data for **8l**: IR (KBr, cm^{-1}): 3427, 2925, 1616, 1448, 1169, 1010. ^1H NMR ($CDCl_3$, 300 MHz): δ 8.05 (d, 2H, J = 7.8 Hz, Ar−H), 7.75 (m, 1H, Ar−H), 7.61 (m, 2H, Ar−H), 7.38 (m, 1H, Ar−H), 7.28 (m, 3H, Ar−H), 5.28 (m, 1H, SCH_2CH), 5.08 (m, 2H, 2 × CH_2CH=CCH_3), 4.58 (t, 2H, J = 5.1 Hz, CH_2O), 3.84 (d, 2H, J = 4.5 Hz, NCH_2), 3.56 (m, 2H, SCH_2), 2.91 (m, 4H, $CON(CH_2)_2$), 2.63 (m, 4H, $N(CH_2)_2$), 1.89−2.04 (m, 8H, 2 × $CHCH_2CH_2CH$), 1.50−1.67 (m, 12H, 4 × CH=CCH_3). MS (ESI) m/z = 695 $[M + 1]^+$. Anal. calcd for $C_{36}H_{46}N_4O_6S_2$: C, 62.22; H, 6.67; N, 8.06. Found: C, 61.95; H, 6.83; N, 7.96.

(*S*)-3-(Phenylsulfonyl)-4-((1-(2-((2*E*,6*E*)-3,7,11-trimethyldodeca-2,6,10-trienylthio)benzoyl)pyrrolidin-2-yl)methoxy)-1,2,5-oxadiazole-2-oxide (8m). The title compound was obtained starting from **1** and **7m**. Colorless viscous liquid, 65% yield. Analytical data for **8m**: $[\alpha]_D^{24}$: −36.4. IR (KBr, cm^{-1}): 3474, 2965, 1630, 1552, 1448, 1169. ^1H NMR ($CDCl_3$, 300 MHz): δ 8.05 (m, 2H, Ar−H), 7.93 (m, 1H, Ar−H), 7.76 (m, 1H, Ar−H), 7.61 (m, 2H, Ar−H), 7.43 (t, 1H, J = 7.2 Hz, Ar−H), 7.39 (m, 1H, Ar−H), 7.29 (m, 1H, Ar−H), 5.19 (m, 1H, SCH_2CH), 5.07 (m, 2H, 2 × CH_2CH=CCH_3), 4.90 (m, 1H, NCH), 4.65 (m, 2H, OCH_2), 3.51 (d, 2H, J = 7.8 Hz, SCH_2), 3.30 (m, 2H, NCH_2), 1.89−2.02 (m, 8H, 2 × $CHCH_2CH_2CH$), 1.50−1.68 (m, 16H, 4 × CH=CCH_3, $CHCH_2CH_2$). MS (ESI) m/z = 666 $[M + 1]^+$. Anal. calcd for $C_{35}H_{43}N_3O_6S_2$: C, 63.13; H, 6.51; N, 6.31. Found: C, 62.95; H, 6.44; N, 6.29.

3-(Phenylsulfonyl)-4-(1-(2-((2*E*,6*E*)-3,7,11-trimethyldodeca-2,6,10-trienylthio)benzoyl)piperidin-4-yloxy)-1,2,5-oxadiazole-2-oxide (8n). The title compound was obtained starting from **1** and **7n**. Colorless viscous liquid, 70% yield. Analytical data for **8n**: IR (KBr, cm^{-1}): 3432, 2929, 1623, 1440, 1285, 1169, 1085. ^1H NMR ($CDCl_3$, 300 MHz): δ 8.05 (m, 2H, Ar−H), 7.77 (t, 1H, J = 7.2 Hz, Ar−H), 7.63 (m, 2H, Ar−H), 7.40 (m, 1H, Ar−H), 7.26 (m, 3H, Ar−H), 5.27 (m, 1H, SCH_2CH), 5.18 (m, 2H, 2 × CH_2CH=CCH_3), 5.08 (m, 1H, OCH), 3.88 (m, 2H, SCH_2), 3.47 (m, 4H, $N(CH_2)_2$), 1.89−2.02 (m, 12H, 2 × $CHCH_2CH_2CH$, $C(CH_2)_2$), 1.50−1.68 (m, 12H, 4 × CH=CCH_3). MS (ESI) m/z = 666 $[M + 1]^+$. Anal. calcd for $C_{35}H_{43}N_3O_6S_2$: C, 63.13; H, 6.51; N, 6.31. Found: 62.88; H, 6.74; N, 6.07.

4-(2-(*N*-(2-Hydroxyethyl)-2-((2*E*,6*E*)-3,7,11-trimethyldodeca-2,6,10-trienylthio)benzamido)ethoxy)-3-(phenylsulfonyl)-1,2,5-oxadiazole-2-oxide (8o). A solution of **1** (0.36 g, 1.00 mmol) and oxalyl chloride (0.5 mL) in dry dichloromethane (5 mL) was stirred at room temperature for 4 h. The solvent was removed under reduced pressure. The crude residue was dissolved in 5 mL of dichloromethane and slowly added to the mixture of **8o** (0.33 g, 1.00 mmol) and triethylamine (0.3 mL) in 10 mL of dichloromethane under an ice bath, and stirring was continued for 12 h. After filtration, the filtrate was evaporated to dryness in vacuo, and the crude product was purified by

column chromatography (PE/EtOAc = 5:1−1:1) to yield as colorless viscous liquid (420 mg, 62%). Analytical data for **8o**: IR (KBr, cm^{-1}): 3450, 1703, 1625, 1548, 1450, 1253, 1171. ^1H NMR ($CDCl_3$, 300 MHz): δ 8.05 (d, 2H, J = 7.8 Hz, Ar−H), 7.75 (m, 1H, Ar−H), 7.61 (m, 2H, Ar−H), 7.38 (m, 1H, Ar−H), 7.28 (m, 3H, Ar−H), 5.28 (m, 1H, SCH_2CH), 5.08 (m, 2H, 2 × $CH_2CH{=}CCH_3$), 4.58 (t, 2H, J = 5.1 Hz, CH_2O), 3.84 (t, 2H, J = 4.5 Hz, NCH_2), 3.56 (m, 2H, SCH_2), 2.91 (m, 3H, CH_2OH), 2.63 (m, 2H, NCH_2), 1.89−2.04 (m, 8H, 2 × $CHCH_2CH_2CH$), 1.50−1.67 (m, 12H, 4 × $CH{=}CCH_3$). MS (ESI) m/z = 670 $[M + 1]^+$. Anal. calcd for $C_{34}H_{43}N_3O_7S_2$: C, 60.96; H, 6.47; N, 6.27. Found: C, 61.12; H, 6.29; N, 6.05.

4,4′-(2,2′-(2-((2*E*,6*E*)-3,7,11-Trimethyldodeca-2,6,10-trienylthio)benzoylazanediyl)bis(ethane-2,1-diyl))bis(oxy) bis(3-(phenylsulfonyl)-1,2,5-oxadiazole-2-oxide) (8p). The title compound was obtained starting from **1** and **7p**. Colorless viscous liquid, 46% yield. Analytical data for **8p**: IR (KBr, cm^{-1}): 2952, 1619, 1554, 1414, 1386, 1164. ^1H NMR ($CDCl_3$, 300 MHz): δ 8.05 (d, 4H, J = 7.5 Hz, Ar−H), 7.79 (t, 2H, J = 7.5 Hz, Ar−H), 7.66 (m, 3H, Ar−H), 7.43 (m, 3H, Ar−H), 7.34 (m, 2H, Ar−H), 5.29 (m, 1H, SCH_2CH), 5.08 (m, 2H, 2 × $CH_2CH{=}CCH_3$), 4.59 (m, 4H, 2 × OCH_2), 3.71 (d, 2H, J = 7.8 Hz, SCH_2), 3.55 (m, 4H, 2 × NCH_2), 1.89−2.02 (m, 8H, 2 × $CHCH_2CH_2CH$), 1.50−1.68 (m, 12H, 4 × $CH{=}CCH_3$). ESI-MS(m/z): 912 $[M + H]^+$. Anal. calcd for $C_{42}H_{47}N_5O_{11}S_3$: C, 56.42; H, 5.30; N, 7.83. Found: C, 56.24; H, 5.55; N, 7.68.

MTT Assay. Individual types of HCC cells at 1 × 10^4 cells/well were cultured 10% fetal calf serum (FCS) DMEM in 96-well microplates overnight. The cells were then treated in triplicate with various concentrations of each compound and cultured in 2% FCS DMEM for 48 h. Control cells were treated with vehicle alone. During the last 4 h of incubation, the cells were exposed to tetrazolium dye (MTT) solution (5 mg/mL, 30 μL per well). The generated formazan crystals were dissolved in 150 μL of dimethyl sulfoxide (DMSO), and the absorbance was read spectrophotometrically at 570 nm using an enzyme-linked immunosorbent assay plate reader. The inhibition of individual compounds on the proliferation of HCC was determined by the formula of 1 − mean OD value of cells treated with compound/mean OD value of control cells, and the IC_{50} was calculated for each compound.

Nitrate/Nitrite Measurement in Vitro. The levels of nitrate/nitrite formed from individual compounds in the cells were determined by the colorimetric assay using the nitrate/nitrite colorimetric assay kit, according to the manufacturer's instructions (Beyotime, China). Briefly, HepG2 and LO2 cells (5× 10^6 cells/well) were treated in triplicate with a 100 μM concentration of one of the compounds (**7l**, **8d**, **8i**, **8j**, **8l**, **8m**, **8o**, and FTS) for 24 h. The cells were harvested and lyzed. The cell lysates were mixed with Griess for 30−300 min, followed by measuring at 540 nm. The cells treated with diluent were used as negative controls for the background levels of nitrate/nitrite production, while sodium nitrate at different concentrations was used as the positive control for the standard curve.

Flow Cytometry Assays. Hep3B and LO2 cells at 1 × 10^6 cells/well were cultured in 10% FCS DMEM overnight and treated in duplicate with 8 μM **8l**, **7l**, FTS, or vehicle alone in 2% FCS DMEM for 48 h, respectively. The cells were harvested and stained with Annexin V and PI (BD PharMigen, San Diego, CA), according to the manufacturers's instruction. Subsequently, the frequency of apoptotic cells was determined by flow cytometry analysis. A total of 1 × 10^4 events were analyzed for each sample, and the percentages of apoptotic cells in each sample were expressed.

Acute Toxicity. Female KM mice were purchased from Shanghai Laboratory Animal Center (SLAC, Shanghai, China) and housed individually in a specific pathogen free facility. Groups of mice (n = 10 per group) were injected intraperitoneally with a single dose 585.9, 468.8, 375.0, 300.0, and 240.0 mg/kg or vehicle control, respectively. The mouse death was monitored daily and recorded up to 14 days post-treatment. The animal experimental protocols were approved by the Animal Research Protection Committee of our campus.

In Vivo Tumor Growth Inhibition. Female BALB/c nude mice at 5−6 weeks of age were from SLAC and inoculated subcutaneously with 10^6 SMMC7721 cells. After solid tumor reached at 100−150 mm^3, the tumor-bearing nude mice were randomized and treated intraperitoneally with, or without, 0.4 mL of vehicle, FTS at 16 mg/kg body weight, and **8l** at 15 or 60 mg/kg daily up to 21 days, respectively. The progression of tumors was monitored every 3 days up to 21 days post-treatment. The tumor volumes were estimated by measuring the two dimensions of the tumors using a caliper in a blinded fashion and calculated by the formula: the volume = 1/2 (length × $width^2$). At the end of the experiment, the mice were sacrificed, and their tumors were dissected out and weighed.

Immunoblotting Assays. Individual tumors were sampled and homogenized (10% w/v) in lysis buffer. After the protein concentrations were determined, individual tumor lysates (50 μg/lane) were separated by sodium dodecyl sulfate−polyacrylamide gel electrophoresis (12% gel) and transferred onto nitrocellulose membranes. After they were blocked with 5% fat-free milk, the target proteins were probed with anti-Akt, antiphospho-Akt (Ser473), anti-ERK, antiphospho-ERK (Thr202/Tyr204), antiphospho-c-Raf (Ser259), and anti-β-actin antibodies (Cell Signaling, Boston, MA), respectively. The bound antibodies were detected by horseradish peroxidase (HRP)-conjugated second antibodies and visualized using the enhanced chemiluminescent reagent. The relative levels of each signaling event to control β-actin were determined by densimetric scanning.

■ ASSOCIATED CONTENT

Supporting Information. Table of compound purity by HPLC. This material is available free of charge via the Internet at http://pubs.acs.org.

■ AUTHOR INFORMATION

Corresponding Author

*Tel: +86-25-83271015. Fax: +86-25-83271015. E-mail: zyhtgd@hotmail.com (Y.Z.). Tel: +86-25-86021369. Fax: +86-25-86635503. E-mail: huijicpu@163.com (H.J.).

Author Contributions

⊥These authors contributed equally to this work.

■ ABBREVIATIONS USED

HCC, human hepatocellular carcinoma; MAPK, mitogen-activated protein kinase; ERK, extracellular signal-regulated kinase; GTP, guanosine triphosphate; FTS, farnesylthiosalicylic acid; NO, nitric oxide; RNS, reactive nitrogen species; ROS, reactive oxygen species; DCC, dicyclohexylcarbodiimide; EDCI, 1-(3-dimethyl aminopropyl)-3-ethylcarbodiimide hydrochloride; DMAP, 4-dimethylaminopyridine; HPLC, high-performance liquid chromatography; SAR, structure−activity relationship; DMSO, dimethyl sulfoxide; PE, petroleum ether

■ REFERENCES

(1) Llovet, J. M.; Bruix, J. Novel advancements in the management of hepatocellular carcinoma in 2008. *J. Hepatol.* **2008**, *48* (Suppl. 1), S20–S37.

(2) Bos, J. L. The ras gene family and human carcinogenesis. *Mutat. Res.* **1988**, *195*, 255–271.

(3) Maity, A.; Pore, N.; Lee, J.; Solomon, D.; O'Rourke, D. M. Epidermal growth factor receptor transcriptionally up-regulates vascular

endothelial growth factor expression in human glioblastoma cells via a pathway involving phosphatidylinositol 3′-kinase and distinct from that induced by hypoxia. *Cancer Res.* **2000**, *60*, 5879–5886.

(4) Porfiri, E.; McCormick, F. Regulation of epidermal growth factor receptor signaling by phosphorylation of the ras exchange factor hSOS1. *J. Biol. Chem.* **1996**, *271*, 5871–5877.

(5) Boguski, M. S.; McCormick, F. Proteins regulating Ras and its relatives. *Nature* **1993**, *366*, 643–654.

(6) Goldberg, L.; Kloog, Y. A Ras inhibitor tilts the balance between Rac and Rho and blocks phosphatidylinositol 3-kinase-dependent glioblastoma cell migration. *Cancer Res.* **2006**, *66*, 11709–11717.

(7) Joneson, T.; White, M. A.; Wigler, M. H.; Bar-Sagi, D. Stimulation of membrane ruffling and MAP kinase activation by distinct effectors of RAS. *Science* **1996**, *271*, 810–812.

(8) Walsh, A. B.; Bar-Sagi, D. Differential activation of the Rac pathway by Ha-Ras and K-Ras. *J. Biol. Chem.* **2001**, *276*, 15609–15615.

(9) Downward, J. Ras signalling and apoptosis. *Curr. Opin. Genet. Dev.* **1998**, *8*, 49–54.

(10) Bos, J. L. Ras oncogenes in human cancer: A review. *Cancer Res.* **1989**, *49*, 4682–4689.

(11) Ogata, N.; Kamimura, T.; Asakura, H. Point mutation, allelic loss and increased methylation of c-Ha-ras gene in human hepatocellular carcinoma. *Hepatology* **1991**, *13*, 31–37.

(12) Richards, C. A.; Short, S. A.; Thorgeirsson, S. S.; Huber, B. E. Characterization of a transforming N-ras gene in the human hepatoma cell line Hep G2: Additional evidence for the importance of c-myc and ras cooperation in hepatocarcinogenesis. *Cancer Res.* **1990**, *50*, 1521–1527.

(13) Yoshida, T.; Hisamoto, T.; Akiba, J.; Koga, H.; Nakamura, K.; Tokunaga, Y.; Hanada, S.; Kumemura, H.; Maeyama, M.; Harada, M.; Ogata, H.; Yano, H.; Kojiro, M.; Ueno, T.; Yoshimura, A.; Sata, M. Spreds, inhibitors of the Ras/ERK signal transduction, are dysregulated in human hepatocellular carcinoma and linked to the malignant phenotype of tumors. *Oncogene* **2006**, *25*, 6056–6066.

(14) Calvisi, D. F.; Ladu, S.; Gorden, A.; Farina, M.; Conner, E. A.; Lee, J. S.; Factor, V. M.; Thorgeirsson, S. S. Ubiquitous activation of Ras and Jak/Stat pathways in human HCC. *Gastroenterology* **2006**, *130*, 1117–1128.

(15) Haklai, R.; Weisz, M. G.; Elad, G.; Paz, A.; Marciano, D.; Egozi, Y.; Ben-Baruch, G.; Kloog, Y. Dislodgment and accelerated degradation of Ras. *Biochemistry* **1998**, *37*, 1306–1314.

(16) Marom, M.; Haklai, R.; Ben-Baruch, G.; Marciano, D.; Egozi, Y.; Kloog, Y. Selective inhibition of Ras-dependent cell growth by farnesylthiosalisylic acid. *J. Biol. Chem.* **1995**, *270*, 22263–22270.

(17) Elad, G.; Paz, A.; Haklai, R.; Marciano, D.; Cox, A.; Kloog, Y. Targeting of K-Ras 4B by S-trans,trans-farnesyl thiosalicylic acid. *Biochim. Biophys. Acta* **1999**, *1452*, 228–242.

(18) Goldberg, L.; Haklai, R.; Bauer, V.; Heiss, A.; Kloog, Y. New derivatives of farnesylthiosalicylic acid (salirasib) for cancer treatment: Farnesylthiosalicylamide inhibits tumor growth in nude mice models. *J. Med. Chem.* **2009**, *52*, 197–205.

(19) Schneider-Merck, T.; Borbath, I.; Charette, N.; De Saeger, C.; Abarca, J.; Leclercq, I.; Horsmans, Y.; Starkel, P. The Ras inhibitor farnesylthiosalicyclic acid (FTS) prevents nodule formation and development of preneoplastic foci of altered hepatocytes in rats. *Eur. J. Cancer* **2009**, *45*, 2050–2060.

(20) Fukuto, J. M.; Wink, D. A. Nitric oxide (NO): Formation and biological roles in mammalian systems. *Met. Ions Biol. Syst.* **1999**, *36*, 547–595.

(21) Millet, A.; Bettaieb, A.; Renaud, F.; Prevotat, L.; Hammann, A.; Solary, E.; Mignotte, B.; Jeannin, J. F. Influence of the nitric oxide donor glyceryl trinitrate on apoptotic pathways in human colon cancer cells. *Gastroenterology* **2002**, *123*, 235–246.

(22) Postovit, L. M.; Adams, M. A.; Lash, G. E.; Heaton, J. P.; Graham, C. H. Nitric oxide-mediated regulation of hypoxia-induced B16F10 melanoma metastasis. *Int. J. Cancer* **2004**, *108*, 47–53.

(23) Dhar, A.; Brindley, J. M.; Stark, C.; Citro, M. L.; Keefer, L. K.; Colburn, N. H. Nitric oxide does not mediate but inhibits transformation and tumor phenotype. *Mol. Cancer Ther.* **2003**, *2*, 1285–1293.

(24) Chen, L.; Zhang, Y.; Kong, X.; Lan, E.; Huang, Z.; Peng, S.; Kaufman, D. L.; Tian, J. Design, synthesis, and antihepatocellular carcinoma activity of nitric oxide releasing derivatives of oleanolic acid. *J. Med. Chem.* **2008**, *51*, 4834–4838.

(25) Maksimovic-Ivanic, D.; Mijatovic, S.; Harhaji, L.; Miljkovic, D.; Dabideen, D.; Fan Cheng, K.; Mangano, K.; Malaponte, G.; Al-Abed, Y.; Libra, M.; Garotta, G.; Nicoletti, F.; Stosic-Grujicic, S. Anticancer properties of the novel nitric oxide-donating compound (S,R)-3-phenyl-4,5-dihydro-5-isoxazole acetic acid-nitric oxide *in vitro* and *in vivo*. *Mol. Cancer Ther.* **2008**, *7*, 510–520.

(26) Moharram, S.; Zhou, A.; Wiebe, L. I.; Knaus, E. E. Design and synthesis of 3′- and 5′-O-(3-benzenesulfonylfuroxan-4-yl)-2′-deoxyuridines: Biological evaluation as hybrid nitric oxide donor-nucleoside anticancer agents. *J. Med. Chem.* **2004**, *47*, 1840–1846.

(27) Huang, Z.; Zhang, Y.; Zhao, L.; Jing, Y.; Lai, Y.; Zhang, L.; Guo, Q.; Yuan, S.; Zhang, J.; Chen, L.; Peng, S.; Tian, J. Synthesis and anti-human hepatocellular carcinoma activity of new nitric oxide-releasing glycosyl derivatives of oleanolic acid. *Org. Biomol. Chem.* **2010**, *8*, 632–639.

(28) Ling, Y.; Ye, X.; Ji, H.; Zhang, Y.; Lai, Y.; Peng, S.; Tian, J. Synthesis and evaluation of nitric oxide-releasing derivatives of farnesylthiosalicylic acid as anti-tumor agents. *Bioorg. Med. Chem.* **2010**, *18*, 3448–3456.

(29) Masumoto, H.; Ohta, S.; Hirobe, M. Application of chemical cytochrome P-450 model systems to studies on drug metabolism: IV Mechanism pathways via an iminium intermediate. Drug. *Metab. Dispos.* **1991**, *19*, 768–780.

(30) Turner, J. M.; Willetts, A. J. Amino ketone formation and aminopropanol-dehydrogenase activity in rat-liver. *Biochem. J.* **1967**, *102*, 511–519.